

# Immunosensor Design Based on Chitosan-QDs, a Nanocomposite-Modified Electrode for Selective Procalcitonin Sensing in Clinic Analyses

## Abstract

A simple free labeled electrochemical immunosensor based on chitosan (CHI) and quantum dots (QDs) was developed for the determination of procalcitonin (ProCT) antigen (Ag) which can act as a target biomarker of infectious diseases. The antibodies of the ProCT biomarker were successfully incubated on the CHI-QDs platform. Electrochemical impedance spectroscopy and cyclic voltammetry were used for the evaluation and characterization of various layers coated onto the electrode. Under the optimum conditions, the electron transfer resistance ( $R_{ct}$ ) of the immunosensor was altered linearly by the ProCT concentration. The proposed immunosensor was proportional to the ProCT biomarker concentration from 0.005 to 0.35 ng/mL with a calculated detection limit of 0.015 pg/mL. The proposed biosensing device also exhibited high stability and reproducibility, which can be used for the quantitative assay of the ProCT biomarker in clinic analyses.

**Keywords:** Carbon paste electrode, Chitosan, electrochemical impedance spectroscopy, immunosensor, quantum dots

## Introduction

Procalcitonin (ProCT) as a hormone calcitonin (CT) precursor helps to adjust the blood calcium level. It is a soluble protein composed of 116 amino acids.<sup>[1]</sup> In healthy people, ProCT is a pro-hormone of CT which is constructed in the thyroid gland via the parafollicular cells (or C-cells), the concentration of its serum being less than 0.05  $\mu\text{g L}^{-1}$ .<sup>[2]</sup> ProCT is the most reliable biomarker in diagnosing and isolating bacterial infections from viral in patients who are admitted for acute reasons such as severe burns, inflammations, surgeries, and respiratory problems. It is also used for early infections in newborn babies in emergency centers and hospitals. By releasing ProCT in the blood, Interferon receptor beta is activated, causing inhibition of the IL-1 beta receptor. This, in turn, makes a difference in bacterial infections which result in sepsis from the viral.<sup>[3-5]</sup> The infections of bacterial attendance in the body result in the emancipation of ProCT in approximately all the cell types and tissues, although the aforementioned process is still not fully understood.<sup>[6]</sup> As a result, after 4h of the infection beginning, the level of ProCT increases dashingly, the phenomenon which has a type of congruity with the intensity of

bacterial infection. Consequently, this causes an enhancement in the ProCT level to over 100  $\mu\text{g L}^{-1}$ , the amount which remains much lower for chronic inflammatory diseases, viral infections, and autoimmune processes.<sup>[7-9]</sup> Evaluation and investigation of the ProCT level in the body can be performed to give the beneficial information to the discernment of infectious from noninfectious disorders in order to barricade the misuse of immense antibiotics to prevent drug resistance to disease. The design of an immunosensor to accurately measure the level of this hormone, using chitosan-quantum dots (CHI-QDs), has been done for the first time in the world. The designed and built immunosensor can be used for prevention, easier control, and better treatment of all the mentioned abnormalities. Accordingly, the discernment of ProCT is very important for valid diagnosis in serum, which can be in effect very contributory to additional therapies.<sup>[10]</sup> In this line, the diverse analytical procedures have been extensively applied. Nonetheless, by considering practical and remarkable endeavors, the selection of a procedure with high sensitivity and good selectivity in diagnosing and analyzing ProCT is yet a problem. To conduct the trial, disparate analytical procedures have been employed for analysis of ProCT, including chemiluminescence immunoassay,<sup>[11]</sup> fluorescence immunoassay,<sup>[12]</sup> immunochromatographic assay,<sup>[13]</sup> ELISA

This is an open access journal, and articles are distributed under the terms of the Creative Commons Attribution-NonCommercial-ShareAlike 4.0 License, which allows others to remix, tweak, and build upon the work non-commercially, as long as appropriate credit is given and the new creations are licensed under the identical terms.

For reprints contact: reprints@medknow.com

**How to cite this article:** Naghizadeh S, Paknejad B, Abtahi SR, Hazrati E, Chamanara M. Immunosensor design based on Chitosan-QDs, a nanocomposite-modified electrode for selective procalcitonin sensing in clinic analyses. *J Rep Pharm Sci* 2021;10:53-9.

Sajad Naghizadeh<sup>1</sup>,  
Babak Paknejad<sup>1</sup>,  
Seyed Reza Abtahi<sup>1</sup>,  
Ebrahim Hazrati<sup>2</sup>,  
Mohsen Chamanara<sup>1</sup>

<sup>1</sup>Department of Pharmacology and Toxicology, Faculty of Medicine, AJA University of Medical Sciences, Tehran, Iran, <sup>2</sup>Department of Anesthesia and Intensive Care, Faculty of Medicine, AJA University of Medical Sciences, Tehran, Iran

Received: 03 Jul 2020  
Accepted: 31 Aug 2020  
Published: 31 May 2021

**Address for correspondence:**  
Mohsen Chamanara, Pharm.  
D/PhD, Department of  
Pharmacology and Toxicology,  
Faculty of Medicine, AJA  
University of Medical Sciences,  
P.O. Box 13145-784, Tehran,  
Iran. Tel: +98 21 43822401;  
fax: +98 21 43822401  
E-mail: Chamanaramohsen@  
gmail.com

## Access this article online

### Website:

www.jrpsjournal.com

DOI:10.4103/jrpts.JRPTPS\_83\_20

### Quick Response Code:



assay,<sup>[14]</sup> and surface plasmon resonance.<sup>[15]</sup> The gradualness in pretreatment steps of the experimental and high cost of examinations by mentioned procedures have caused them not to be proper for normal analysis. Therefore, the choice of a substitute procedure accompanied by lower operating cost and effective detection speed for assessment the low level of ProCT is a challenging endeavor. According to this view, using the immunoassay procedures, as a hopeful procedure, was offered.

Immunoassay procedures are used as considerable diagnosis procedures in environmental, biochemical, and clinical evaluations as well as in food industries. These are performed by the feature of selective distinction of Ag by antibody (Ab) based on electrochemical, optical, or gravimetric methods.<sup>[16-18]</sup> Electrochemical immunosensors have impressive features due to their simplicity of construction, their improvements in the development of portable and affordable devices, and good sensitivity.<sup>[19,20]</sup> To this purpose, nanostructures and nanotechnology, owing to their extraordinary physicochemical properties, have recently been utilized in the field in order to enhance the analytical operation of the electrochemical immunoassay procedures.<sup>[21,22]</sup>

QDs, due to the quantum confinement effect and the extent of their energy band gap, have useful optical and electrical properties. QDs in electrochemical sensors can facilitate the electron transfer speed. As a result, these materials are employed widely as the amplifier of the signal element in electrochemical and electroluminescence sensors, owing to their unique properties.<sup>[23]</sup> In addition, QDs have widespread utilization in biological and medical applications as immunoassay since they can well bind to biorecognition molecules.<sup>[24,25]</sup>

In this regard, CHI with a good film-forming ability, stability, biocompatibility, and strong adherence to the electrode surface could be mixed with QDs and used as a carbon past modifier. Following the discovery of the QDs, they have been effectively used as sensing materials<sup>[26,27]</sup> in modified electrodes, which might be due to their high electrical conductivity, electrocatalytic activity, and good biocompatibility.

In line with the previous research in the field, and to add further to the present knowledge, this experimental study was conducted in which a sensitive free-labeled electrochemical immunosensory is employed to measure ProCT in serum samples of a number of patients. In this regard, the ProCT Ab was immobilized on the transfer surface. The CHI-QD nanocomposite is placed on this transfer platform, the platform used for enhancing electrochemical signal and stability sensor. To detect resistance changes accurately, the proposed immunosensors were placed in a biomarker solution.

## Experimental

### Apparatus and measurements

An Autolab system potentiostat–galvanostat model PGSTAT 214 (Utrecht, The Netherlands) using a NOVA (1.11) software

was exerted to all the electrochemical experiments, which were carried out at room temperature. A platinum wire and a silver–silver chloride (Ag/AgCl, 3 M KCl) electrodes were utilized as auxiliary and reference electrodes, respectively. Electrochemical impedance spectroscopy (EIS) with an FRA 32 impedance analysis module and cyclic voltammetry (CV) experiments were performed by Ab/CHI-QDs/CPE as a working electrode. All pH measurements were performed by Metrohm pH-meter, Model 691 that was equipped with a glass electrode during the experiments. To evaluate the manufactured immunosensor surface morphology, the method of the scanning electron microscope (SEM) (Philips XL 30) was employed. In these experiments, the EURONDA (EUROSONIC 4D model) was utilized to disperse the particles inside the solution and its uniformity.

### Substances

*N*-Hydroxy succinimide (NHS) and *N*-ethyl-*N*-[3-dimethylaminopropyl] carbodiimide (EDC) from the Sigma-Aldrich (Munich, Germany), graphite powder of Fluka Co. (Buchs, Switzerland), CHI potassium ferricyanide, and paraffin oil of Merck Co. (Darmstadt, Germany) were purchased. All aqueous solutions were prepared with double-distilled water. ProCT Ag and ProCT Ab or anti-ProCT were purchased from Medical Biology Research Center, Kermanshah University of Medical Sciences (Kermanshah, Iran). All other chemicals used in the present experiment were prepared from Merck Co., Germany, and were of adequate analytical purity. In the experiments, phosphate-buffered solutions (PBS) (0.1 M) at various pH values were prepared by 0.1 M H<sub>3</sub>PO<sub>4</sub>, 0.1 M KH<sub>2</sub>PO<sub>4</sub>, and 0.1 M K<sub>2</sub>HPO<sub>4</sub>. Sodium hydroxide (NaOH) and hydrochloric acid (HCl) solutions were used for the adjustment of buffer solutions' pH. In the first step, the ProCT and its Ab were frozen, and their standard solutions were constructed for fresh use day after day. Next, the serum samples of some patients were collected from Imam Reza Hospital (Kermanshah, Iran). All experiments were accomplished at the ambient temperature. The additional chemicals and reagents consumed in the present research were acquired as analytical grade and applied without additional purification.

### Synthesis of QDs

To synthesize the QDs, the previously established methods have been applied.<sup>[28]</sup> First, sodium hydrogen telluride (NaHTe) was prepared by reducing Te powder with sodium borohydride (NaBH<sub>4</sub>) in deionized water under stirring conditions along with N<sub>2</sub> purging. After 3 h, the produced NaHTe was used to prepare the particles of CdTe. In another flask, 0.3 g of CdCl<sub>2</sub>·H<sub>2</sub>O was dissolved in 40 mL of ultrapure water followed by the addition of 200 μL of TGA, while the solution was stirred intensely. The pH of the reaction was adjusted to 10 by adding dropwise of NaOH solution (1 M). In the next step, the freshly prepared NaHTe was added to a CdCl<sub>2</sub> solution containing TGA under N<sub>2</sub> atmosphere. Following mixing, the solution was transferred into a Teflon-lined stainless-steel autoclave and heated in an oven at 120°C for 3 h. Then, the autoclave was cooled and thiol-capped CdTe QDs were obtained.

## Preparing the immunosensor

The order of procedure for immunosensor making is depicted in Scheme 1. To construct the mentioned immunosensor, the first carbon paste electrode (CPE) was constructed by using the paraffin oil and analytical grade graphite powder in a 30:70 (%w/w) ratio. This composite was blended inside a mortar to form a completely homogeneous mixture. The obtained paste was pressed in a PVC tube and blocked on the side which had an electrical connection with a copper wire passing through the center of the electrode body.

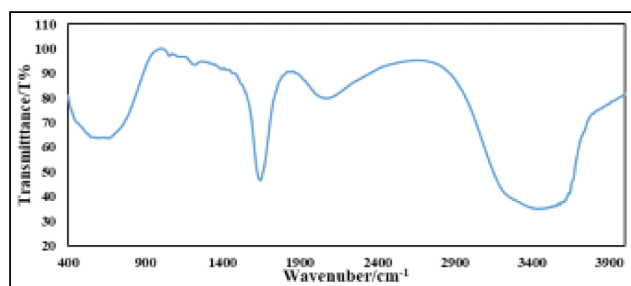
Then the formed electrode was put at room temperature to be dried for 1 day. Afterward, the CHI-QD nanocomposite was prepared by direct mixing of 0.2 mg of CHI, 20  $\mu\text{L}$  of QDs in 10 mL of DMSO, and the resulted suspension was ultrasonically homogenized. Next 4.0  $\mu\text{L}$  of suspension was dropped onto the surface of the CPE and was allowed to be dried at room temperature.

To activate the sensor surface of functional groups, this sensor was dipped in the solution containing 3 mL of 100 mM NHS and 1 mL of 50 mM EDC for 2 h and washed with double distilled water. Next, the Ab/CHI-QDs/CPE was prepared by dipping the CHI-QDs/CPE into the Ab solution (anti-ProCT) and kept at 4°C for 5 h to react at room temperature. The fabricated electrode was kept overnight at 4°C and saturated moisture. The obtained electrode was eventually rinsed with a PBS solution of pH 7.5 to eliminate excessive physically adsorbed Ab. Afterward, 15  $\mu\text{L}$  of 10 g L<sup>-1</sup> HSA in the PBS was added to block the residual active sites on the working electrode. Following this, the immunosensor was washed with a buffer solution. To retain from an immobilized Ab activity, the prepared immunosensor was held at 4°C into the buffer solution.

## Scheme 1

### Preparing the human blood serum

Serum instances of 10 patients were collected from Imam Reza Hospital (Kermanshah, Iran) and stored frozen until it was analyzed. Then 1 mL of saturated ammonium sulfate solution as serum protein precipitating agent was appended into the centrifuge tubes containing serum samples. After being vortexed for 15 min, the precipitated protein was separated by centrifugation at 15,000 rpm. The clear supernatant layer was



Scheme 1: The schematic illustration for construction of immunosensor

filtrated by a filter with a size of 0.45  $\mu\text{m}$  Millipore to produce a protein-free blood serum.

## Results and Discussion

### Characterization of CdTe QDs

FT-IR spectroscopy was performed to investigate the functional groups of the QDs. [Figure S1], Scheme 1 shows the characteristic peaks of TGA-capped CdTe QDs. The absorption peaks at 1643  $\text{cm}^{-1}$  are due to the symmetric and asymmetric stretching of the carboxylate group. Bands at 1222 and 3421  $\text{cm}^{-1}$  are the stretching vibration of C–O and O–H, respectively.

### The appraisal of the surface features of the various fabricated electrodes

The physical morphologies of the sensors are affected by their outcomes. Therefore, in the first stage, the difference between the structures of the designed electrode surfaces at each step was examined by the SEM method. The forms of SEM of the CPE (A) and CHI-QDs/CP B(C) are illustrated in Figure 1. The energy-dispersive X-ray spectroscopy (EDX) image is shown in Figure 1C. The EDX indicates the presence of different percentages of C, O, Cd, and Te at the prepared composite electrode.

### Electrochemical characterization of the immunosensor

The CV and EIS methods have been widely employed to study the interface properties of different electrode surfaces. As shown in Figure 2A and B, CV and Nyquist plots of CPE (curve a), CHI/CPE (curve b), and CHI-QDs/CP were recorded.

The peak currents at the CPE (curve a) have the lowest and highest values of currents. As can be seen, the current response at the surface of CPE (curve a) is rather poor. Following the anchoring of CHI on CPE, the CHI electrode exhibited a much lower interfacial charge transfer resistance for the occurred redox reaction [Figure 2A, curve b]. When QDs were attached to CHI/CPE [Figure 2A, curve c], it supplied a great impressive surface area due to its conductivity, as it contrasted with the signals at the CPE [Figure 2A, curve c]. So, next to attaching the colloidal QDs at the electrode surface to form CHI-QDs/CPE [Figure 2A, curve c], the current response of the marker redox was depicted to be more enhanced than the CHI/CPE. Furthermore, QDs, through enhancement in the performance of further electron transfer between the target and the electrode surface, operated as nano-sized electrodes.

Even so, after immobilization of Ab at the surface of CHI-QDs/CP to form (Ab/CHI-QDs/CP/CPE), the related CV [Figure 2A, curve d] results in a decrease in current signal, as well as an increase in the differentiation between the anodic and cathodic waves of the redox marker. This observation demonstrated that the rate of electron-transfer of the  $[\text{Fe}(\text{CN})_6]^{3-/4-}$  system was reduced, owing to the attendance of Ab at the surface of electrode. In fact, following the immobilization of the Ag, the

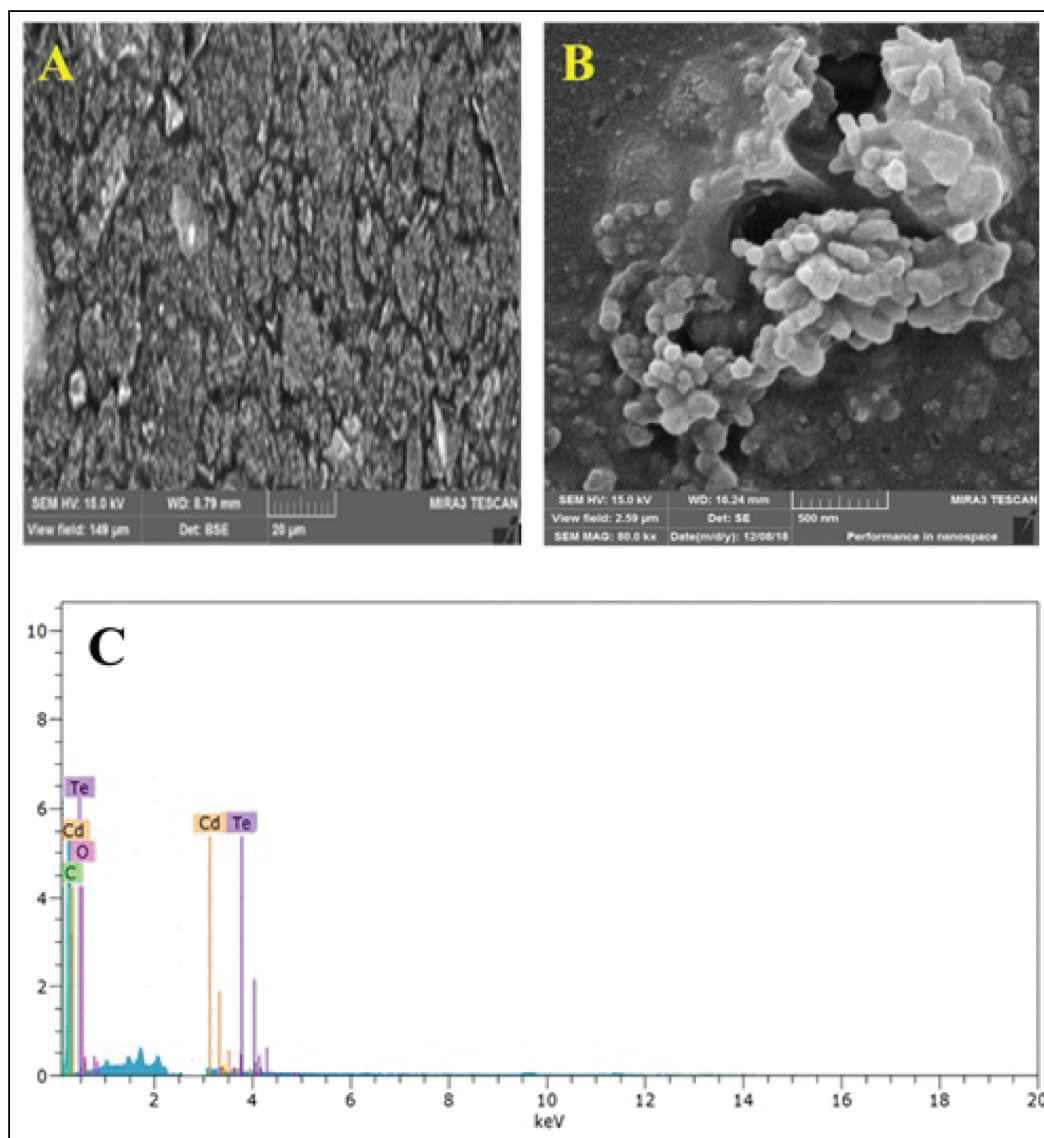


Figure 1: SEM images of CPE (A) and CHI-QDs/CPE (B). EDX spectrum is illustrated (C)

conductivity of the modified electrode declined [Figure 2A, curve e], resulting in the formation of adduct between Ab and Ag on the surface of the designed sensor. This created Ab–Ag as an approximately inert blocking layer on the electron transfer rate and barricaded the diffusion of the redox probe to the surface of the electrode.

EIS is further used to study the interfacial characterization of the different modified electrodes. The diameter of the semicircle usually equals to the electron transfer resistance ( $R_{et}$ ) and occurs in lower frequencies. Electron transfer resistance ( $R_{et}$ ) controls the electron transfer kinetics of the redox probe at the electrode interface which commonly showed the faradaic process at the interface of electrode/electrolyte. An electrical circuit was depicted based on the features of the obtained impedance spectrum. The straight line of the Nyquist plots appeared at lower frequencies, which corresponded to the diffusion process of the electroactive species from solution to electrode interface (Warburg element,  $W$ ).<sup>[29]</sup>

Figure 2B shows the acquired impedance spectra during the step-by-step modification process. As it is seen, the CHI/CPE [Figure 2A, curve b] electrode disclosed the smaller semicircle domain than CPE [Figure 2B, curve a], suggesting that the redox probe has a lower electron-transfer resistance against CHI owing to their conductivity. Subsequent to the deposition of the composite of QDs at the CHI/CPE surface [Figure 2B, curve c], the  $R_{et}$  value decreased compared to CHI/CPE with the higher conductivity of the CHI/CPE. However, when the QDs was supplied a great conductive layer role on the CNFs film, the interfacial electron transfer between solution and electrode was increased. After immobilization of the Ab on the surface of CHI-QDs/CPE to form Ab/CHI-QDs/CPE through EDC/NHS linker, the electron transfer resistance of the system increased through the confining of an interfacial electron transfer [Figure 2B, curve d]. This was owing to an insulating characteristic of the protein layer at the surface of the constructed electrode, and led to greater electron transfer resistance, which ultimately resulted in the enlargement of the

semicircle in the related Nyquist plot [Figure 2A, curve e]. Also, due to the formation of Ab–Ag adduct as a primary ineffective and insulated electron transfer, blocking layer at the surface of constructed immunosensor can mainly barricade the diffusion of the redox probe to the surface of the designed sensor [Figure 2A, curve e]. The acquired outcomes from the EIS and CV measurements were compatible with each other.

### Analytical conditions optimization

To obtain increased sensitivity and the analytical performance immunosensor, the effective parameters of the proposed immunosensor including the concentration/time of Ab included on an electrode and the incubation time of ProCT whit Ab were evaluated.

To optimize the immobilization of Ab concentration, solutions containing different concentrations of the Ab were immobilized on CHI-QDs/CPE. Figure S2A shows the effect of the immobilization of Ab concentration at the surface electrode modified with the response. As a result, the Ab concentration was optimized at 30  $\mu\text{g}/\text{mL}$  with the highest resistance, which allows the sensitive detection of ProCT. No change was observed in the resistance signal of more than 30  $\mu\text{g}/$

mL of Ab concentration. Also, Ab incubation time to CHI-QDs/CPE played an important role in sensor functioning as, in the low incubation time, a weak connection between the Ab and the CHI-QDs/CPE is established. Therefore, it was removed before the measurement. As shown in Figure S2B, the maximum signal of the measurement was observed at an incubation time of 50 min.

To use the maximum capacity of the immunosensor, the incubation different times between ProCT and Ab were investigated. The result of the investigation is summarized in Figure S2C. The highest signal is observed at 50 min. Thus, the 50-min period as the best incubation time between antibodies and biomarkers was selected.

### Analytical performance

The analytical performance of the proposed immunosensor in the various concentrations of the ProCT was assessed by the Nyquist plot. Following the incubation in various ProCT concentrations for 50 min, the Nyquist plots were recorded in the solution comprised of the  $[\text{Fe}(\text{CN})_6]^{3-/4-}$  (5.0 mM) and KCl (0.1 M). As shown in Figure 3, with an increase in the biomarker concentration, the  $R_{ct}$  increase was proportionally observed and the linear relationship between signal responses and the ProCT concentration was obtained in the concentration range of 0.005–0.35 ng/mL. The calibration curve with a regression equation of  $R/\Omega = 650.89 [C_{\text{ProCT}}/\text{ngml}^{-1}] + 203.06$  ( $R^2 = 0.9859$ ) and the detection limit (DL) was calculated

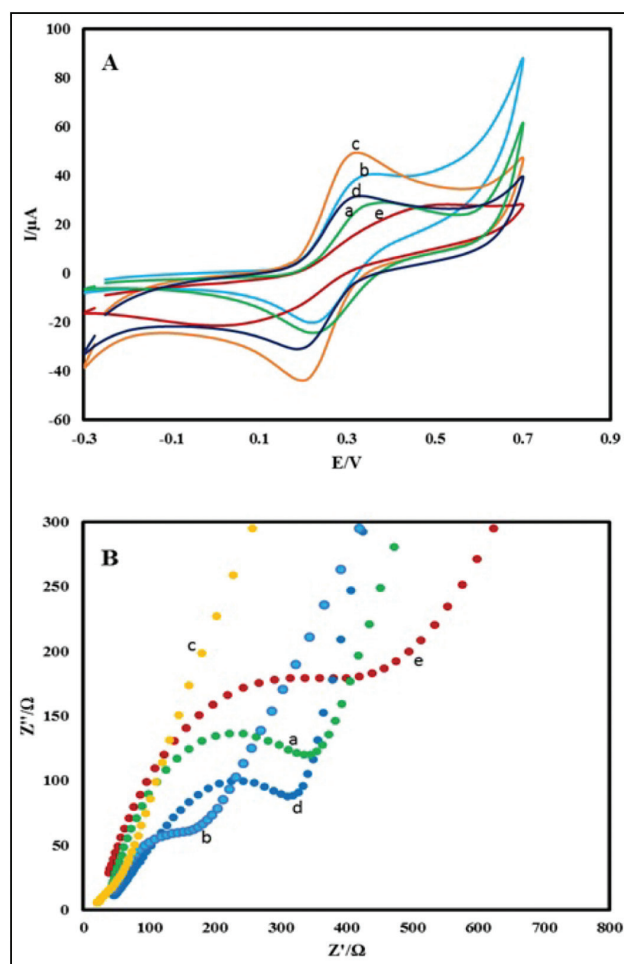


Figure 2: Cyclic voltammograms (A) and Nyquist diagrams (B) recorded in the solution 0.1 M KCl, 0.5 mM  $[\text{Fe}(\text{CN})_6]^{3/4-}$  for CPE (a), CHI/CPE (b), CHI-QDs/CPE (c), Ab/CHI-QDs/CPE (d), Ab–Ag/CHI-QDs/CPE

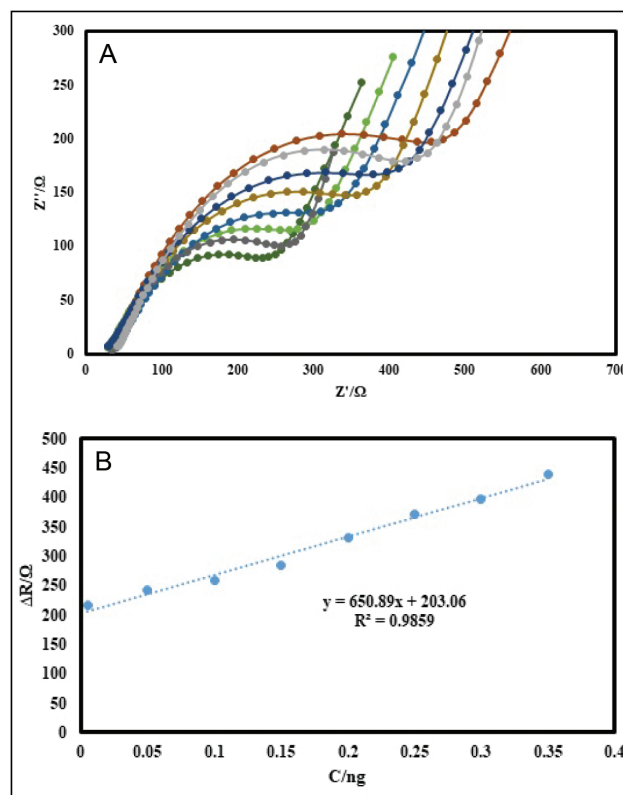


Figure 3: (A) The EIS of Ab/CHI-QDs/CPE recorded in different concentrations of ProCT. (B) The plot of  $\Delta R_{ct}$  vs  $[\text{ProCT}]$  over the concentration range of 0.005–0.35 ng/mL. Inset shows the signal relates to with  $[\text{ProCT}]$

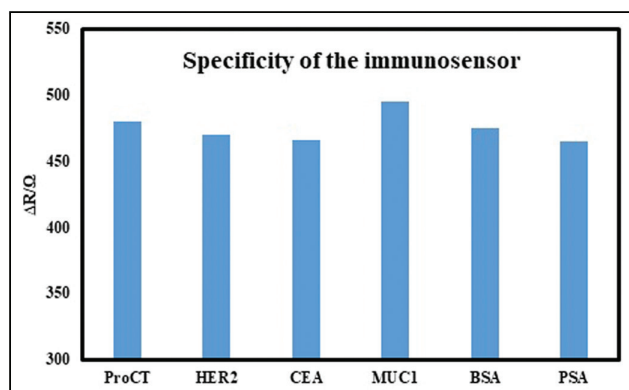


Figure 4: Selectivity of the immunosensor. The  $\Delta R_{ct}$  of the immunosensor in the presence of 0.1 ng/mL ProCT and various interference (10 ng/mL)

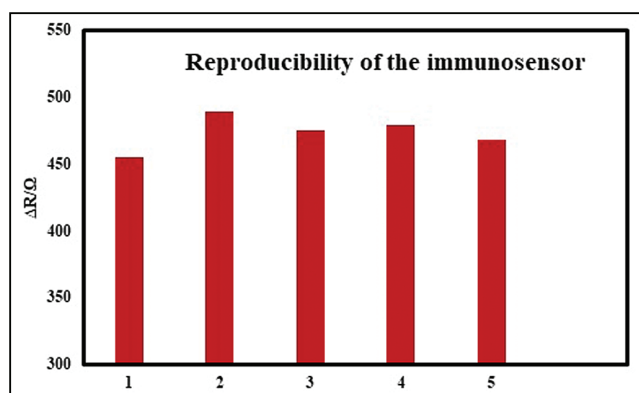


Figure 5: EIS response of sensors to different electrodes treated in the same conditions

based on  $3S_b/m$ , where  $3S_b$  is within three standard deviations of the blank signals and  $m$  is the slope of the calibration curve as 0.015 pg/mL.

### Specificity of the immunosensor

The ability of the specificity of the presented immunosensor using HER2, CEA, MUC1, and BSA as the interference was investigated. The response of the 10 ng/mL of interference solution with the 0.1 ng/mL of ProCT is demonstrated in Figure 4. As seen, the signal interference observed was less than 10%, indicating the specificity of the label-free electrochemical immunosensor which can be regarded as acceptable. The unknown biomarker concentration is obtained using a standardized method.

### Reproducibility and stability of immunosensor

The intra-assay reproducibility was investigated by consecutive measurements of 0.1 ng/mL of ProCT for five times using the Ab/CHI-QDs/CPE independently. The average relative standard deviation (RSD) of the five individually constructed electrodes was 2.7%. This indicates that the immunosensor had acceptable reproducibility [Figure 5].

One of the most important and critical parameters in evaluating the performance and progression of immunosensors is determining their long-term stability. Next to preparing the

Table 1: Determination of ProCT in real blood samples

Sample	Measured concentration by immunosensor (ng/mL)	Recovery (%)
1	60.2	107.5
2	24.5	90.7
3	68.7	95.5
4	101.2	106.5

immunosensor and storing it at 4°C, the offered immunosensor maintained 88% of its primary activity after being stored for 15 days, which shows the stability of this proposed electrode. Therefore, the finding illustrated the good long-term stability to immunosensor in the discernment of ProCT.

### Real sample analysis

The accuracy of blood samples in the hospital was evaluated by the proposed electrochemical immunosensor. The serum samples were obtained from three healthy persons. Then, following the addition of different concentrations of ProCT into healthy human serum samples, the standard addition method was applied to measure the ProCT using the EIS method.

Consequently, to test the accuracy of the offered immunosensor, a commercially stock kit (ELISA Quantitation kit) was employed as a standard. According to the ELISA kits manufacturer, the reactivity of these kits is susceptible to operator and factor changes such as washing methods, composite types of the reagents, incubation temperature, and time, as well as other empirical factors. The results are presented in Table 1. As it is depicted from the result, the recovery of ProCT was found to be between 90 and 107.5%, which manifests the good precision of the method for ProCT monitoring using the proposed immunosensor. This means that this electrochemical immunosensor provided a potential application for the analysis of ProCT in real samples.

### Conclusions

In the present research, a new free-type electrochemical immunosensor was introduced for the highly accurate detection of ProCT based on deposition of CHI, QDs, and Ab at the CPE surface. In sensor architecture, the unique properties of CHI and QDs were used to stabilize the Ab. The immobilized Ab probe could well track the ProCT. The proposed immunosensor could respond with a linear range from 0.005 to  $-0.35$  ng/mL, with the detection limit of 0.015 pg/mL. The acquired data illustrated adequate sensitivity and simplicity of this procedure for ProCT detection in the serum samples with good accuracy and reproducibility. It can be expected that the offered immunosensor can be employed extensively for sensitive clinical and biological diagnoses and applications.

### Financial support and sponsorship

Nil.

### Conflicts of interest

Authors declare that they have no conflicts of interest.

## References

- Pierrakos C, Vincent JL. Sepsis biomarkers: A review. *Crit Care* 2010;14:R15.
- Krämer PM, Kess M, Kremmer E, Schulte-Hostede S. Multi-parameter determination of TNF $\alpha$ , PCT and CRP for point-of-care testing. *Analyst* 2011;136:692-5.
- Nelson GE, Mave V, Gupta A. Biomarkers for sepsis: A review with special attention to India. *Biomed Res Int* 2014;2014:264351.
- Becker KL, Snider R, Nylen ES. Procalcitonin in sepsis and systemic inflammation: A harmful biomarker and a therapeutic target. *Br J Pharmacol* 2010;159:253-64.
- Christ-Carin M. Procalcitonin in bacterial infections-hype, hope, more or less? *Swiss Medical Weekly* 2005;135:451-60.
- Müller B, White JC, Nylén ES, Snider RH, Becker KL, Habener JF. Ubiquitous expression of the calcitonin-I gene in multiple tissues in response to sepsis. *J Clin Endocrinol Metab* 2001;86:396-404.
- Deis JN, Creech CB, Estrada CM, Abramo TJ. Procalcitonin as a marker of severe bacterial infection in children in the emergency department. *Pediatr Emerg Care* 2010;26:51-60; quiz 61-3.
- Wacker C, Prkno A, Brunkhorst FM, Schlattmann P. Procalcitonin as a diagnostic marker for sepsis: A systematic review and meta-analysis. *Lancet Infect Dis* 2013;13:426-35.
- van Rossum AM, Wulkan RW, Oudesluys-Murphy AM. Procalcitonin as an early marker of infection in neonates and children. *Lancet Infect Dis* 2004;4:620-30.
- Fang YS, Wang HY, Wang LS, Wang JF. Electrochemical immunoassay for procalcitonin antigen detection based on signal amplification strategy of multiple nanocomposites. *Biosens Bioelectron* 2014;51:310-6.
- Hubl W, Krassler J, Zingler C, Pertschy A, Hentschel J, Gerhards-Reich C, *et al.* Evaluation of a fully automated procalcitonin chemiluminescence immunoassay. *Clin Lab* 2003;49:319-27.
- Baldini F, Bolzoni L, Giannetti A, Porro G, Senesi F, Trono C. A fluorescent immunoassay for the determination of procalcitonin and C-reactive protein. *Proc SPIE* 7356, *Optical Sensors 2009*, 735613 (18 May 2009). doi: 10.1117/12.821005.
- Shao X-Y, Wang C-R, Xie C-M, Wang X-G, Liang R-L, Xu W-W. Rapid and sensitive lateral flow immunoassay method for procalcitonin (PCT) based on time-resolved immunochromatography. *Sensors* 2017;17:480.
- Kremmer E, Meyer K, Grässer FA, Flatley A, Kösters M, Lippa PB, *et al.* A new strategy for the development of monoclonal antibodies for the determination of human procalcitonin in serum samples. *Anal Bioanal Chem* 2012;402:989-95.
- Sener G, Ozgur E, Rad AY, Uzun L, Say R, Denizli A. Rapid real-time detection of procalcitonin using a microcontact imprinted surface plasmon resonance biosensor. *Analyst* 2013;138:6422-8.
- Lippa PB, Sokoll LJ, Chan DW. Immunosensors—principles and applications to clinical chemistry. *Clin Chim Acta* 2001;314:1-26.
- Heineman WR, Halsall HB. Strategies for electrochemical immunoassay. *Anal Chem* 1985;57:1321A-31A.
- Ricci F, Adornetto G, Palleschi G. A review of experimental aspects of electrochemical immunosensors. *Electrochim Acta* 2012;84:74-83.
- Li X-M, Yang X-Y, Zhang S-S. Electrochemical enzyme immunoassay using model labels. *TrAC Trends Anal Chem* 2008;27:543-53.
- Wei MY, Wen SD, Yang XQ, Guo LH. Development of redox-labeled electrochemical immunoassay for polycyclic aromatic hydrocarbons with controlled surface modification and catalytic voltammetric detection. *Biosens Bioelectron* 2009;24:2909-14.
- Moon JM, Kim YH, Cho Y. A nanowire-based label-free immunosensor: Direct incorporation of a PSA antibody in electropolymerized polypyrrole. *Biosens Bioelectron* 2014;57:157-61.
- Jang HD, Kim SK, Chang H, Choi J-W. 3D label-free prostate specific antigen (PSA) immunosensor based on graphene-gold composites. *Biosens Bioelectron* 2015;63:546-51.
- Pedrero M, Campuzano S, Pingarrón JM. Quantum dots as components of electrochemical sensing platforms for the detection of environmental and food pollutants: A review. *J AOAC Int* 2017;100:950-61.
- Chandan H, Schiffman JD, Balakrishna RG. Quantum dots as fluorescent probes: Synthesis, surface chemistry, energy transfer mechanisms, and applications. *Sensors Actuat B* 2018;258:1191-214.
- Bozrova S, Baryshnikova M, Sokolova Z, Nabiev I, Sukhanova A. In vitro cytotoxicity of CdSe/ZnS quantum dots and their interaction with biological systems. *KnE Energy Phys* 2018;3:58-63.
- Amelia M, Lincheneau C, Silvi S, Credi A. Electrochemical properties of CdSe and CdTe quantum dots. *Chem Soc Rev* 2012;41:5728-43.
- Li CC, Hu J, Lu M, Zhang CY. Quantum dot-based electrochemical biosensor for stripping voltammetric detection of telomerase at the single-cell level. *Biosens Bioelectron* 2018;122:51-7.
- Manikandan M, Francis PN, Dhanuskodi S, Maheswari N, Muralidharan G. High performance supercapacitor behavior of hydrothermally synthesized CdTe nanorods. *J Mater Sci Mater Electron* 2018;29:17397-404.
- Huang H, Liu Z, Yang X. Application of electrochemical impedance spectroscopy for monitoring allergen-antibody reactions using gold nanoparticle-based biomolecular immobilization method. *Anal Biochem* 2006;356:208-14.

## Supplementary Materials

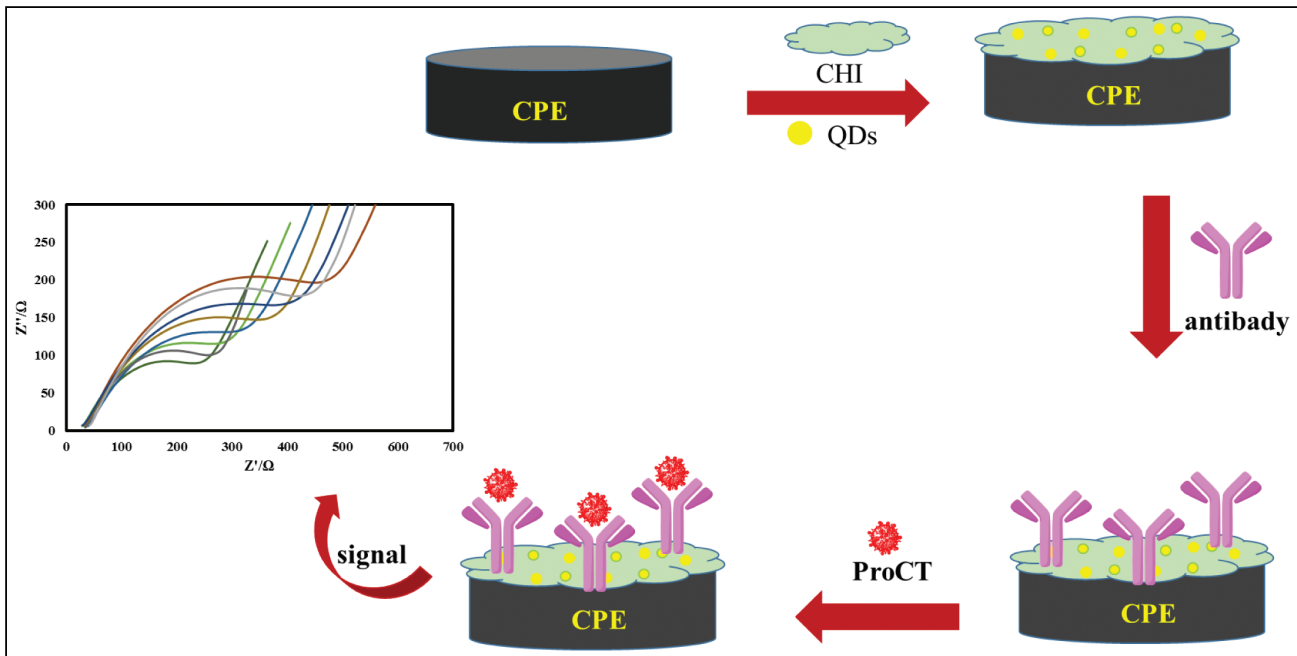


Figure S1: FT-IR spectrum of QDs. (A) Optimization of the incubation concentration of Ab. (B) Optimization of the incubation time of Ab. (C) Optimization of the incubation time of ProCT with Ab



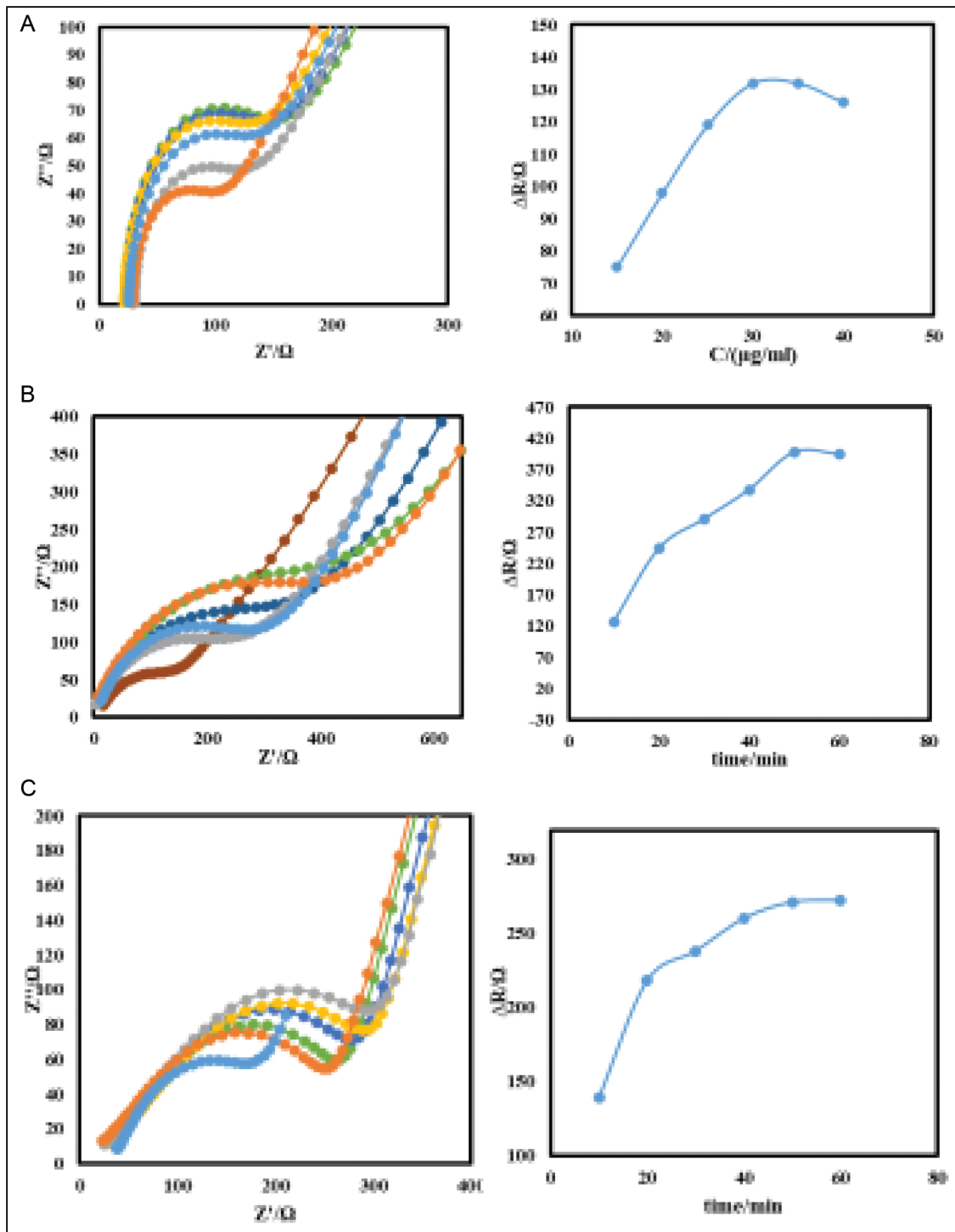


Figure S2: The EIS of Ab/CHI-QDs/CPE recorded in different optimization steps. (A and B) Incubation concentration and an incubation time of the Ab, and (C) incubation time of the incubation times between ProCT and Ab in a solution of 0.1 M PBS at pH 7.